Environ. Sci. Technol. **2002**, *36,* 468−476

Evidence for a Dynamic Cycle between Mn and Co in the Water Column of a Stratified Lake

MARTIAL TAILLEFERT,*,†,‡
BARBARA J. MACGREGOR,†,§
JEAN-FRANÇOIS GAILLARD,†
CHARLES-PHILIPPE LIENEMANN,||,⊥
DIDIER PERRET,||,# AND
DAVID A. STAHL†,▽

Department of Civil Engineering, Northwestern University, Evanston, Illinois 60208, School of Earth & Atmospheric Sciences, Georgia Institute of Technology, Atlanta, Georgia 30332, Max Planck Institute for Marine Microbiology, Celsiusstrasse 1, D-28359 Bremen, Germany, Institut de Chimie Minérale et Analytique, Université de Lausanne, CH-1015 Lausanne, Switzerland, Department of Rural Engineering, Swiss Federal Institute of Technology, CH-1015 Lausanne, Switzerland, and Department of Civil and Environmental Engineering, University of Washington, Seattle, Washington 98195

The geochemical behavior of Co in aquatic systems has often been related to the presence of Fe and Mn particles. A few studies have shown that Co is exclusively associated with particulate Mn, but the dynamics of Co and Mn cycling have never been determined in real time under natural conditions. In this study, we used a combination of analytical techniques to study the temporal and spatial evolution of Mn microparticles (MnO_x) over 2 weeks in the water column of a shallow stratified lake (Paul Lake, MI). We report a temporal accumulation of dissolved Mn at the oxic−anoxic transition, and we show that this accumulation is due to the reductive dissolution of Mn particles. The reductant has not been identified, but abiotic reduction by $\sum H_2S$ and ferrous iron is excluded because they are produced below the zone of MnO_x reduction. Hybridization of RNA isolated from Paul Lake with oligonucleotide probes targeting the δ proteobacteria, which include metal-reducing species, suggests that their activity is greatest at and just below the oxic−anoxic transition, so that Mn reduction may be influenced by bacterial activity. Mn-oxidizing bacteria were isolated from this zone as well. We also demonstrate that the dynamic evolution of MnO_x has a direct influence on the distribution of Co in the water column of this lake: dissolved Co is released during the reductive dissolution of MnO_x and accumulates at the redox interface.

* Corresponding author phone: (404)894-6043; fax: (404)894-5638; e-mail: mtaillef@eas.gatech.edu.
† Northwestern University.
‡ Georgia Institute of Technology.
§ Max Planck Institute for Marine Microbiology.
|| Université de Lausanne.
⊥ Present address: Institut Français du Pétrole, F-69390 Vernaison, France.
Swiss Federal Institute of Technology.
▽ University of Washington.

Introduction

Beginning with the pioneering work of Morgan (*1*), the Mn cycle in aquatic systems has been well-studied over the years. Under oxidizing conditions, Mn exists in the form of a wide variety of minerals including feitknechtite, a Mn(III) mineral (β-MnOOH) (*2*), and numerous polymorphic MnO_2 minerals, e.g., vernadite (δ-MnO_2) (*3*−*5*); these may include foreign ions, e.g., birnessite ($Na_4Mn_{14}O_{27}{\cdot}9H_2O$) (*3*, *6*). These authigenic minerals, synthesized by biotic or abiotic processes in the presence of oxygen, are characterized by mixed Mn oxidation states and are usually reduced under anoxic conditions.

The oxygenic oxidation of Mn^{2+}, although thermodynamically favorable in the pH range of natural waters, is very slow (*7*, *8*), and catalysts such as hydrous oxides (*9*) or microorganisms (*10*−*13*) are needed for the reaction to proceed efficiently. Because of this slow oxidation rate, Mn^{2+} can diffuse through the oxic−anoxic interface, and MnO_x may form within the oxic zone (e.g., refs *14*−*16*). However, it has been shown that the oxidation of Mn^{2+} could occur by denitrification below the oxygen minimum if nitrate is present (*17*). This could prevent MnO_x formation in the oxic zone.

Manganese oxides are strong oxidants and easily reduced in anoxic conditions (*18*). However, parameters such as light intensity and pH (*19*, *20*); availability of dissolved organic reductants (*19*, *21*), Fe^{2+} (*22*, *23*), and reduced sulfur (*23*, *24*); assimilation by microorganisms (*24*−*26*); sorption by inorganic phases (*27*); and precipitation of carbonate phases (*28*, *29*) control the release of Mn^{2+}. More recently, it has been proposed that the reduction of MnO_x may occur by anoxygenic oxidation of ammonium (*17*, *30*). The kinetics of MnO_x reduction has generally been studied in the laboratory (*19*, *21*, *22*, *24*), while a dynamic cycle of Mn has been observed on a seasonal basis in aquatic systems (*4*, *23*). To our knowledge, short-term changes in the distribution of Mn have never been observed in a natural environment.

Cobalt, as the central metal cofactor in vitamin B_{12}, is an essential micronutrient for phytoplankton growth (*31*) and is involved in the biomethylation of heavy metals (*32*). The geochemical behavior of Co in aquatic systems is often related to the presence and oxidation state of Mn (*15*, *33*−*38*). Several studies have shown that Co is sorbed by MnO_x (*34*−*36*) and can be oxidized to Co(III) during this process (*35*, *36*). The mechanism is still uncertain: it has been shown that Co oxidation occurs during the bacterially mediated oxidation of Mn^{2+} (*37*, *38*), even in the absence of Mn^{2+} (*38*), or during the reduction of MnO_2 if Co is complexed by a weak-field ligand (*39*). It has also been demonstrated that Co could be oxidized to Co(III) by reduction of the extremely reactive Mn(III) to Mn^{2+} at the surface of Mn(III)-rich minerals (*40*). In a previous investigation of submicron particles in the water column of a stratified lake (Paul Lake, MI), we showed that MnO_x were associated with bacteria and that these Mn crusts were carrying a significant amount of Co (*15*). Although the recycling of trace metals in the dissolved phase is largely driven by the dissolution of their carrying host, including MnO_x (*15*, *33*), this process has never been directly observed in a natural system.

In this new study, we observed the reductive dissolution of MnO_x in the oxic−anoxic transition during a 2-week period and the concomitant release of Co in the dissolved phase. We present here results relevant to the partitioning of Co and Mn between the dissolved and the particulate phases, as obtained by two complementary analytical tools: Zeeman graphite furnace atomic absorption spectrometry (GFAAS)

10.1021/es010915t CCC: $22.00 © 2002 American Chemical Society
Published on Web 01/04/2002

and analytical electron microscopy. In addition, we present preliminary molecular and microbiological evidence for the presence of microbes that could be involved in the Mn cycle.

Experimental Section

Site Description. This study was conducted in Paul Lake, a small lake located in UNDERC (University of Notre Dame Environmental Research Center) at the border of Wisconsin and the Upper Peninsula of Michigan (46°13′ N and 89°32′ W). Paul Lake is a brown-water kettle lake surrounded on three sides by moraine ridges (*41*) with a surface area of 1.2 ha, a mean depth of 5.0 m, and a maximum depth of approximately 12 m. Its protected location and high depth to surface area ratio help maintain stratification (*42*), although complete mixing has been reported at least once (*43*). Paul Lake is considered mesotrophic (*44*). The concentration of soluble reactive phosphorus in the surface water is very low (ca. 50 nM), but nutrient regeneration at the oxic−anoxic transition promotes phytoplankton blooms just above this interface (*42*). Light can penetrate the top of the chemocline, allowing bacterial photosynthesis (*45*) on a seasonal basis (*41*, *46*).

Sampling and Chemical Analysis. The water column chemistry and microbiology of Paul Lake were investigated in July−August 1996. The physical and chemical characteristics of Paul Lake were established using a portable CTD−pH−O_2 probe (Scout, Hydrolab) calibrated appropriately (*47*). Water samples were collected every 50 cm by peristaltic pump (Cole Parmer) with Tygon tubing. The samples were retrieved in line, i.e., without contact with the atmosphere, using polypropylene syringes (HSW). When required, the waters were subsequently filtered through 0.45-μm Acrodisc LC-PVDF Gelman filters. Generally, samples were kept in the syringes under N_2 atmosphere and at 4 °C until analysis within 30 min after sampling (Fe^{2+}, H_2S), but aliquots were preserved in polypropylene tubes (Falcon) acidified with HNO_3 for the analysis of Mn and Co and in unacidified tubes for the analysis of SO_4^{2-}. The sampling equipment and containers were cleaned with trace metal grade HNO_3 (Fisher Scientifics) and Milli-Q water (Millipore).

Sulfate was determined by capillary electrophoresis (CIA, Waters), and $\sum H_2S$ (= H_2S + HS^- + S^{2-}) and Fe^{2+} were measured colorimetrically using a homemade flow injection analysis instrument and the methylene blue (*48*) and ferrozine (*49*) methods, respectively. Dissolved manganese, determined as total dissolved manganese (Mn_d) in filtered samples, and total manganese (Mn_t), determined in unfiltered samples, were measured by GFAAS (Varian AA800). Total cobalt (Co_t) and total dissolved cobalt (Co_d) were measured by GFAAS using a double injection technique to enhance sensitivity (*15*). The detection limit, reported within a confidence interval of 3σ, was 1.8 nM for Mn and 1.0 nM for Co. Particulate manganese (Mn_p) was measured using three different methods: (i) the difference method, i.e., $Mn_p = Mn_t - Mn_d$; (ii) the filter digestion method, i.e., depending on the depth investigated, between 245 and 580 mL of water was filtered online through a 0.2-μm Schleicher-Schüll cellulose acetate filter, and the filter was digested in a mixture of 0.2 M trace metal HNO_3 and 0.1 M $NH_2OH{\cdot}HCl$ for 24 h at 25 °C; and (iii) a colorimetric method to determine reactive MnO_x in unfiltered samples (*50*), i.e., Mn complexation with 4,4′,4″-methylidynetris[*N*,*N*-dimethylaniline] to produce a crystal violet dye. For the latter, Mn_p standards were diluted from a stock solution freshly prepared with a mixture of 20 mM $MnCl_2$ and 18 mM $KMnO_4$ solutions at neutral pH. The concentration of Mn_p was then determined by addition of an excess of KI in acidic conditions, followed by back-titration of the released iodine with a standard solution of 6 mM $Na_2S_2O_3$. Similar concentrations of particulate Mn were measured by the three methods, suggesting that filtration was not creating significant artifacts and that particulate Mn essentially consists of reactive MnO_x.

Transmission Electron Microscopy Analyses. Bulk water samples were collected with 50-mL syringes (HSW) from 2 to 9 m, with a depth resolution of 0.25 m between 4.5 and 8 and of 0.5 m for the other depths. Sealed syringes were transferred to a N_2-purged glovebag and prepared for transmission electron microscopy-energy dispersive spectroscopy (TEM-EDS) analysis, using a nondisturbing procedure, within 10 min after sampling (*15*). A turbidity-dependent volume of the sample was ultracentrifuged (Beckman Optima TLX with swing-out rotor TLS-55) above TEM copper grids (collodion coated, carbon covered) to collect submicron particles. The supernatant was carefully withdrawn under N_2 atmosphere, and TEM grids were post-protected (*51*) with a thin film of hydrophilic resin (Nanoplast FB101 (*52*)). Grids were visualized by TEM (Zeiss EM10, 80 kV), and the elemental analysis of individual entities were performed by TEM-EDS (Hitachi HF-2000, 200 kV; windowless Noran detector; counting time, 80−300 s; nominal magnification of 150,000; probe size of ca. 3 nm; CIME, EPF Lausanne; see details of the procedure in refs *15* and *47*).

Ribosomal RNA (rRNA) Extraction and Hybridization. Oligonucleotide probes targeting δ proteobacterial groups known to include metal reducers were used to measure concentrations of small-subunit ribosomal RNA (SSU rRNA), a component of the RNA−protein complex responsible for translation of messenger RNA into protein. The evolution of SSU rRNA has paralleled the evolution of species, so sequence comparisons can be used to infer phylogenetic relationships. Probes targeting more- or less-conserved regions of the sequence can be designed to measure RNA concentrations at resolutions from the universal down to the genus or even species level. Because cellular rRNA production tends to increase with growth rate and extracellular RNA is quickly degraded, relative SSU rRNA concentrations in a sample reflect the composition of the active community (*53*). The main objective of the molecular study was to relate general microbial distribution using domain-level oligonucleotide probes to Mn cycling in this lake. It is difficult to use phylogenetic analyses to assign a specific physiological function such as Mn reduction, and the key microbial species contributing to Mn reduction in aquatic systems have not yet been identified. However, species capable of Mn as well as Fe reduction are targeted by the probes specific for δ proteobacteria used in this study. As described for the filter digestion method above, samples were collected by filtering between 160 and 410 mL of waters (depending on the depth investigated) onto 0.4-μm Isopore membranes (Millipore). The material was rinsed from filters by vortexing with 2 mL of sterile Milli-Q water. rRNA was extracted by bead beating, phenol−chloroform extraction, and ethanol precipitation; transferred to nylon membranes; and probed with radiolabeled oligonucleotides as previously described (*54*, *55*). Oligonucleotides (Operon Technologies, Inc.) were named by Oligonucleotide Probe Database conventions (*56*). Universal probe (S-*-Univ-1390-a-A-18 (*57*)) hybridization was compared to total domain-level probe hybridization (Bacteria, S-D-Bact-0338-a-A-18 (*58*); Eukarya, S-D-Euca-1379-a-A-16 (*59*); Archaea, S-D-Arch-0915-a-A-20 (*60*)). Two probes targeting δ proteobacteria were also used (S-F-Dsv-0687-a-A-16 and S-*-Dsb-0804-a-A-18 (*61*)). Membranes were prehybridized at 40 °C and washed at 44 (S-*-Univ-1390-a-A-18; S-F-Dsv-0687-a-A-16), 56 (S-D-Arch-0915-a-A-20), 54 °C (S-D-Bact-0338-a-A-18), 42 (S-D-Euca-1379-a-A-16), or 46 °C (S-*-Dsb-0804-a-A-18). Hybridization was measured with a PhosphorImager (model 400S; Molecular Dynamics Inc.).

Isolation of Mn-Oxidizing Bacteria. Columns packed with sterile sand were percolated for 10 days with water collected at 5.25 m in Paul Lake to allow colonization. Columns were

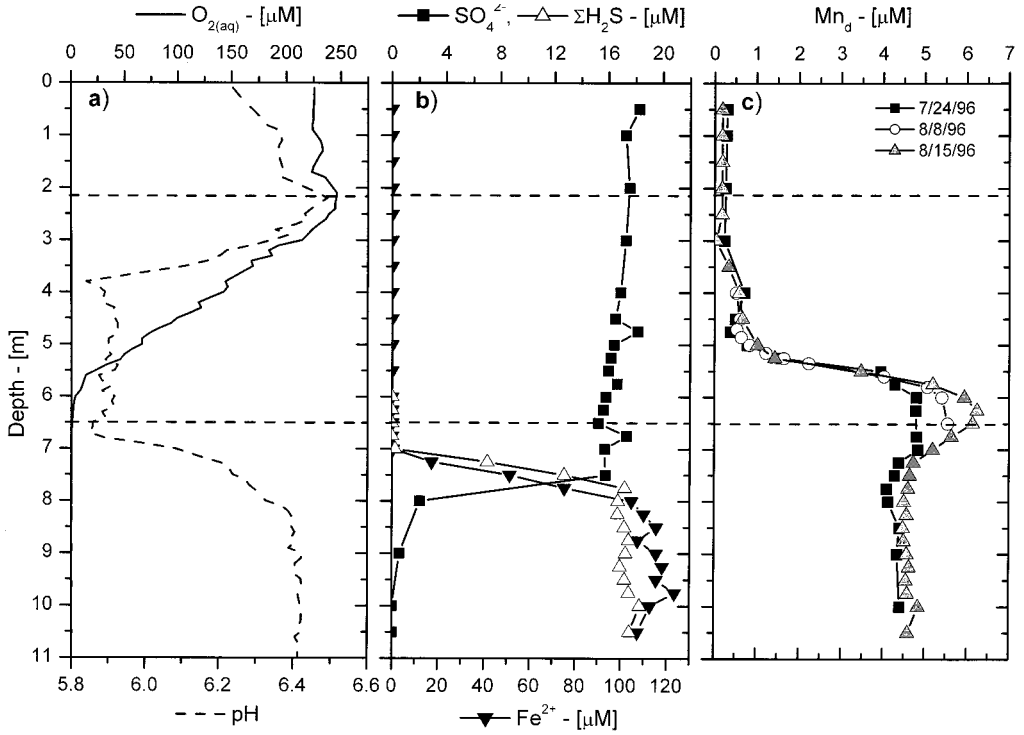

FIGURE 1. Chemical profiles collected in the water column of Paul Lake: (a) O_2(aq) and pH on July 27, 1996; (b) SO_4^{2-}, ΣH_2S, and Fe^{2+} on July 24, 1996; and (c) dissolved manganese (Mn_d) on July 24, August 8, and August 15, 1996. The dashed lines indicate the location of the chemocline, i.e., maximum and minimum oxygen concentration.

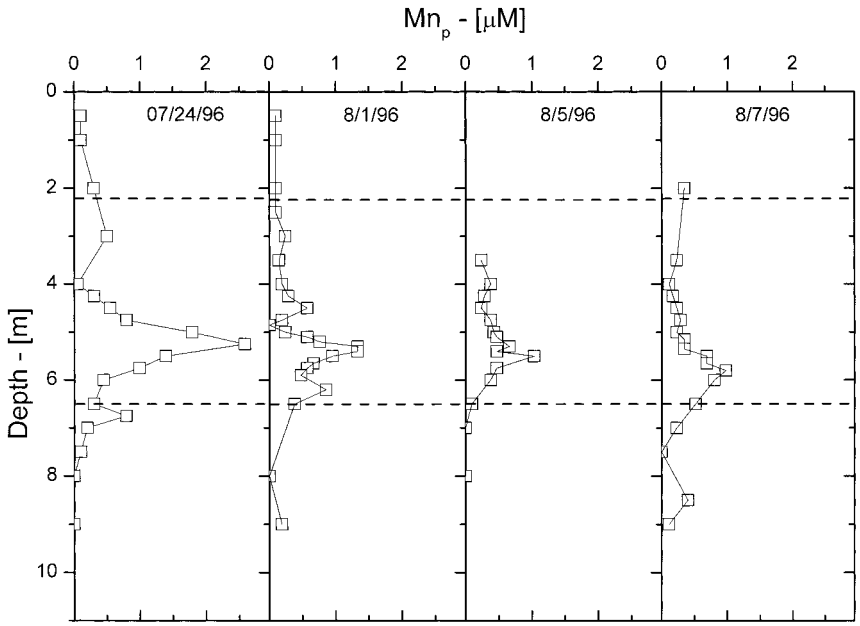

FIGURE 2. Profiles of particulate manganese (Mn_p) in the water column of Paul Lake collected over a period of 2 weeks from July 24 to August 7, 1996. The dashed lines indicate the location of the chemocline.

then percolated for 4 weeks with a sterile, low organic nutrient medium, supplemented with a 100 μM Mn^{2+} solution in HEPES. After 3 weeks, a brown deposit was visible in the outlet tubing, which was chemically identified by TEM-EDS as manganese oxide. No such deposits were observed in control columns that were not inoculated. At the end of the experiment, bacteria were desorbed from the columns with a chemical dispersant (*62*) for isolation and viable counts (*63*).

Results and Discussion

Solution Chemistry. A strong stratification with an oxic–anoxic transition extending from 2.2 m (the depth of maximum O_2(aq)) to 6.5 m (the depth of minimum O_2(aq)) was observed (Figure 1a). This stratification results from oxygen respiration in the water column and a low oxygen supply below 2.2 m during the summer season. Dissolved oxygen is at saturation at the lake surface (225 μM) but increases to 245 μM at 2.2 m during photosynthesis (Figure

1a). Because the summer of 1996 was particularly cold and humid, the production of oxygen by photosynthesis was 40−60% lower than observed in previous spring and summer seasons (*15*, *46*, *47*). The pH profile reflects photosynthesis in the upper water column and respiration in the chemocline: the pH increases from 6.2 at the surface of the lake to 6.4 at the photosynthetic maximum, decreases during respiration to 5.8 at 3.8 m, and remains constant throughout the chemocline (Figure 1b). Below 6.7 m, the pH increases again to 6.4 at 8.3 m and seems to be buffered around the pK_a of the carbonate system below that depth. Sulfate is constant at around 16 μM from the surface to 7.5 m, then decreases sharply to 2 μM at 8 m, and is below detection limit at 10 m (Figure1b). Sulfate reduction simultaneously produces $\sum H_2S$ below 7 m, which reaches a maximum of ca. 17 μM at 7.75 m and remains constant below that. Similarly, Fe^{2+} is below detection limit above 7 m and increases between 7 and 8 m to 105−110 μM deeper (Figure 1b). Finally, Mn_d is generally low (<1 μM) and constant from the surface of the lake to 4.75 m, at which depth Mn_d increases sharply to 4.75 μM at 6 m on July 24 to 5.48 μM at 6.5 m on August 8 and to 6.2 μM at 6.25 m on August 15 (Figure 1c). Although data were not collected below 6.5 m on August 8, Mn_d generally decreases to around 4.5 μM below 7.25 m. These data clearly show that Mn_d is produced in the lower part of the chemocline during a 2-week period.

Dissolution of MnO_x. The profiles of Mn_p measured over the same 2-week period show a well-defined peak of Mn_p in the middle of the chemocline with a maximum concentration of 2.6 μM on July 24 (Figure 2a). These data show that Mn^{2+} oxidation occurs immediately below the oxygen maximum. However, the Mn_p maximum concentration decreases from 2.6 μM on July 24 to 1.3 μM on August 1 (Figure 2b), to 1.0 μM on August 5 (Figure 2c), and to 0.9 μM on August 7 (Figure 2d), confirming that Mn particles are reduced in the chemocline during these 2 weeks. In addition, the Mn_p maximum seems to descend in the water column (Figure 2), suggesting that particles sink during this period. In contrast to the summer of 1995 (*15*), the bacteria observed at the Mn_p maximum (Figure 3a) are not Mn-encrusted, as confirmed by TEM-EDS analysis. However, four manganese-oxidizing bacterial strains were isolated from these 1996 samples. Mn-oxidizing bacteria are widely distributed among the proteobacteria (Figure 4) and other microbial lineages. Isolate 23 is a γ proteobacterium, closely affiliated with manganese-oxidizing *Pseudomonas putida* strains. The remaining isolates are β proteobacteria. While this group includes manganese-oxidizing strains of *Leptothrix* and *Sphaerotilus*, the isolates from Paul Lake belong to a separate lineage (Figure 4) from which to our knowledge no other metal oxidizers have yet been identified.

Between 5.75 and 6 m, aggregates containing Mn-rich material similar to that observed in 1995 (*15*) are present (see arrows in Figure 3b). These TEM-EDS observations at the microparticle level that show MnO_x at 5.75 m (Figure 3b) but not at 5.25 m (Figure 3a) on August 5, 1996, are in agreement with the bulk chemistry data (Figure 2), strengthening the evidence that production of MnO_x at the surface of bacteria is probably inhibited in August 1996 and that MnO_x particles have settled to 5.75 m, where they are reduced. The pH and O_2(aq) concentrations are much lower between 4 and 6.5 m (Figure 1a) than in our previous study in July 1995 (*15*), indicating that the rate of formation of MnO_x, proportional to both pH and O_2(aq) (*8*), is much slower in 1996 or even null.

It has been shown that a higher light intensity and lower pH can facilitate Mn^{2+} production (*19*, *20*). The pH influences rates of reductive dissolution through its impact on the chemical speciation of reductants, oxide surface sites, and reaction intermediates (*19*). Indeed, we observe a Mn_d maximum (Figure 1c) and Mn_p dissolution (Figure 2) in the pH minimum zone. Inorganic reductants such as H_2S and Fe^{2+} may reduce hydrous manganese oxides (*22*−*24*). The reduction of MnO_x is even faster with Fe^{2+} than H_2S (*23*), although stoichiometrically more MnO_x can be reduced by H_2S than by Fe^{2+} (*24*). These reactions could explain the absence of Mn particles below the chemocline (Figure 2), where $\sum H_2S$ and Fe^{2+} are present (Figure 1b), but cannot explain the reductive dissolution of MnO_x between 4.75 and 6.5 m. Alternatively, the disappearance of Mn_p could be due to their nonreductive dissolution to colloidal Mn (not retained by 0.45-μm filters). However, we were unable to observe by TEM-EDS Mn particles below 6 m (*66*), which suggests that the reductive dissolution of MnO_x is accomplished within the chemocline only. Recently, it has been proposed that

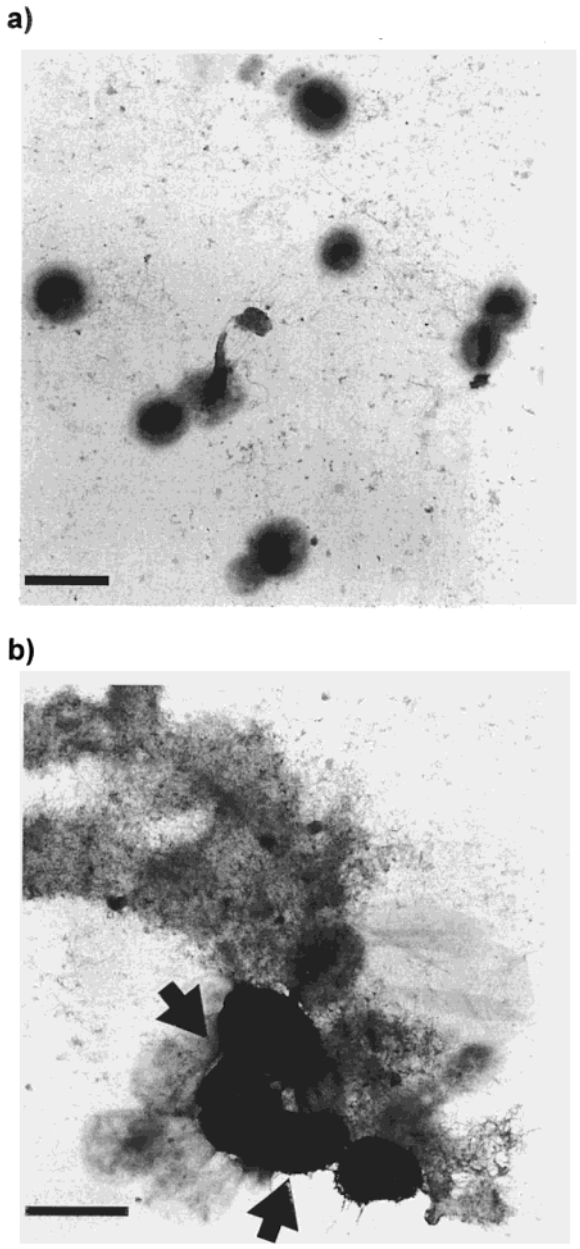

FIGURE 3. Transmission electron micrograph showing (a) bacteria at 5.25 m in the water column of Paul Lake on August 5, 1996. No Mn overgrowth is detected by EDS at the surface of these bacteria. (b) Aggregates containing Mn (located by the arrows) at 5.75 m. These observations are in good agreement with the bulk chemistry data of Figure 2 that show little MnO_x at 5.25 m and a maximum MnO_x at 5.75 m on August 5, 1996. Scale bar = 1 μm.

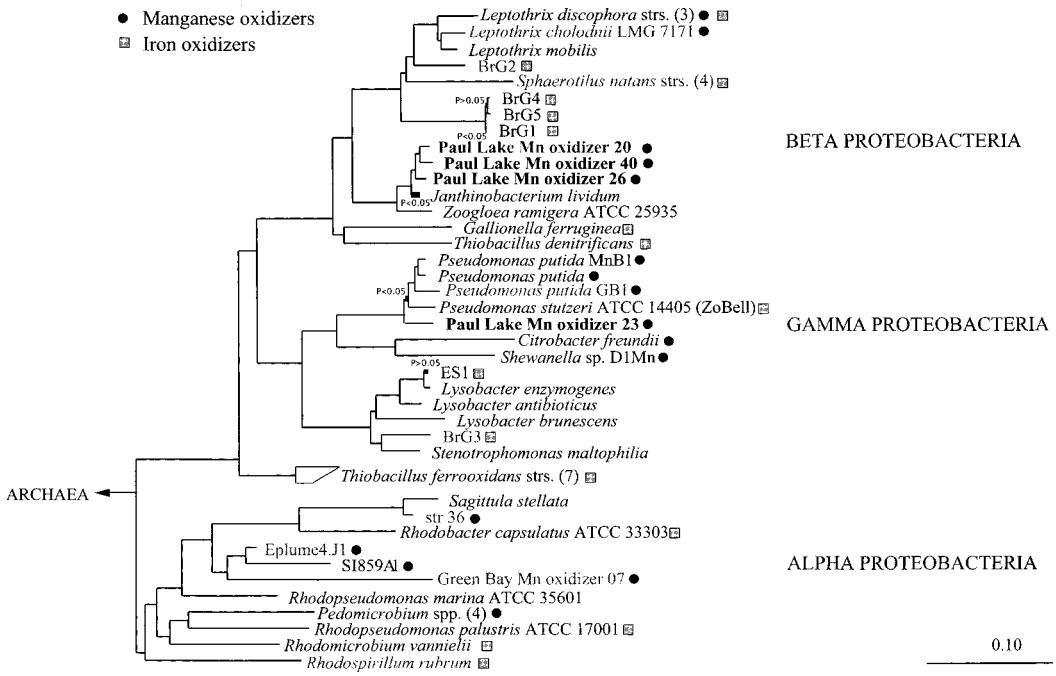

FIGURE 4. 16S rDNA phylogeny of Mn-oxidizing Paul Lake isolates. The tree includes the closest relatives of Paul Lake sequences as well as currently recognized Mn- and Fe-oxidizing bacteria among the β, γ, and α proteobacteria. The tree was constructed using FastDNA ML, including only positions that were similar in 40% or more of the sequences shown in black (*64*). All branch lengths were significant ($P < 0.01$) with the exceptions indicated. Shorter partial sequences, shown in gray, were added by maximum parsimony. The scale bar represents 0.1 base changes per position. Numbers in parentheses indicate the number of sequences combined in a single branch. Green Bay Mn oxidizer 07 was isolated from Lake Michigan sediments (*65*).

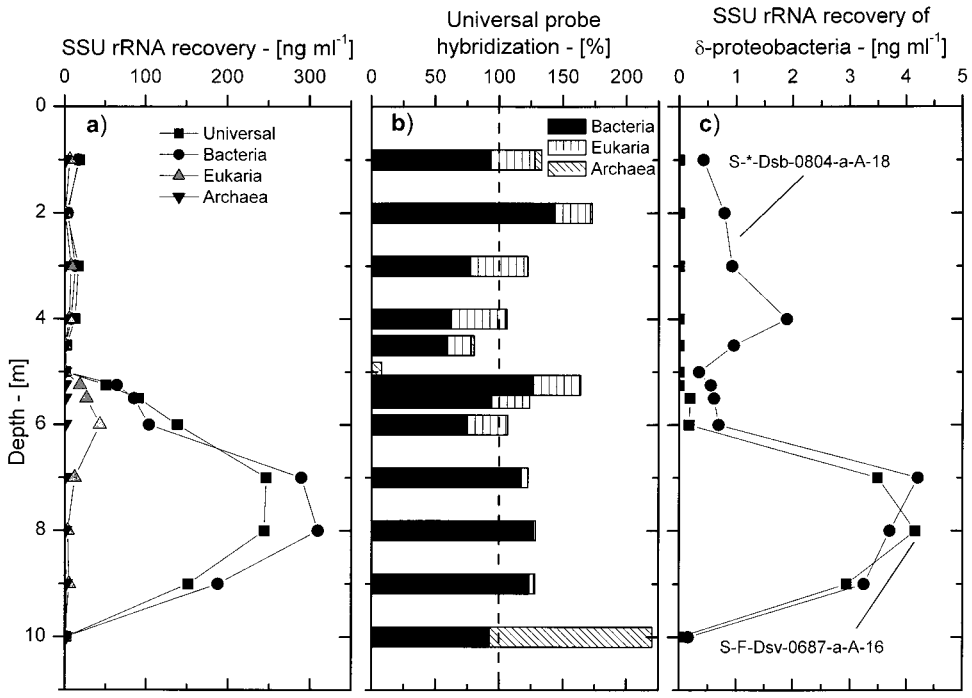

FIGURE 5. Depth profiles of (a) SSU rRNA recovery in ng of rRNA/mL of filtered sample for the universal probe (S-*-Univ-1390-a-A-18) and the three domain probes (bacterial, S-D-Bact-0338-a-A-18; eukaryotic, S-D-Euca-1379-a-A-16; archaeal, S-D-Arch-0915-a-A-20); (b) domain summations in percent of the universal probe; and (c) δ proteobacteria-specific probes (S-F-Dsv-0687-a-A-16 and S-*-Dsb-0804-a-A-18) in ng of rRNA/mL of filtered sample.

MnO_x reduction can occur by anoxygenic NH_4^+ oxidation (*17*, *30*). The exact conditions favoring this reaction are still unknown (*67*), but the pH is low enough (*17*) for it to occur (Figure 1a). Unfortunately, NH_4^+ was not measured in 1996. However, NH_4^+ was present in the lower end of the chemocline in July 1995 (not shown), suggesting that this reaction may take place.

Mn-Reducing Bacteria. SSU rRNA profiles (in nanograms of rRNA per milliliter of filtered sample) are shown in Figure 5a for the universal probe compared to the summation of

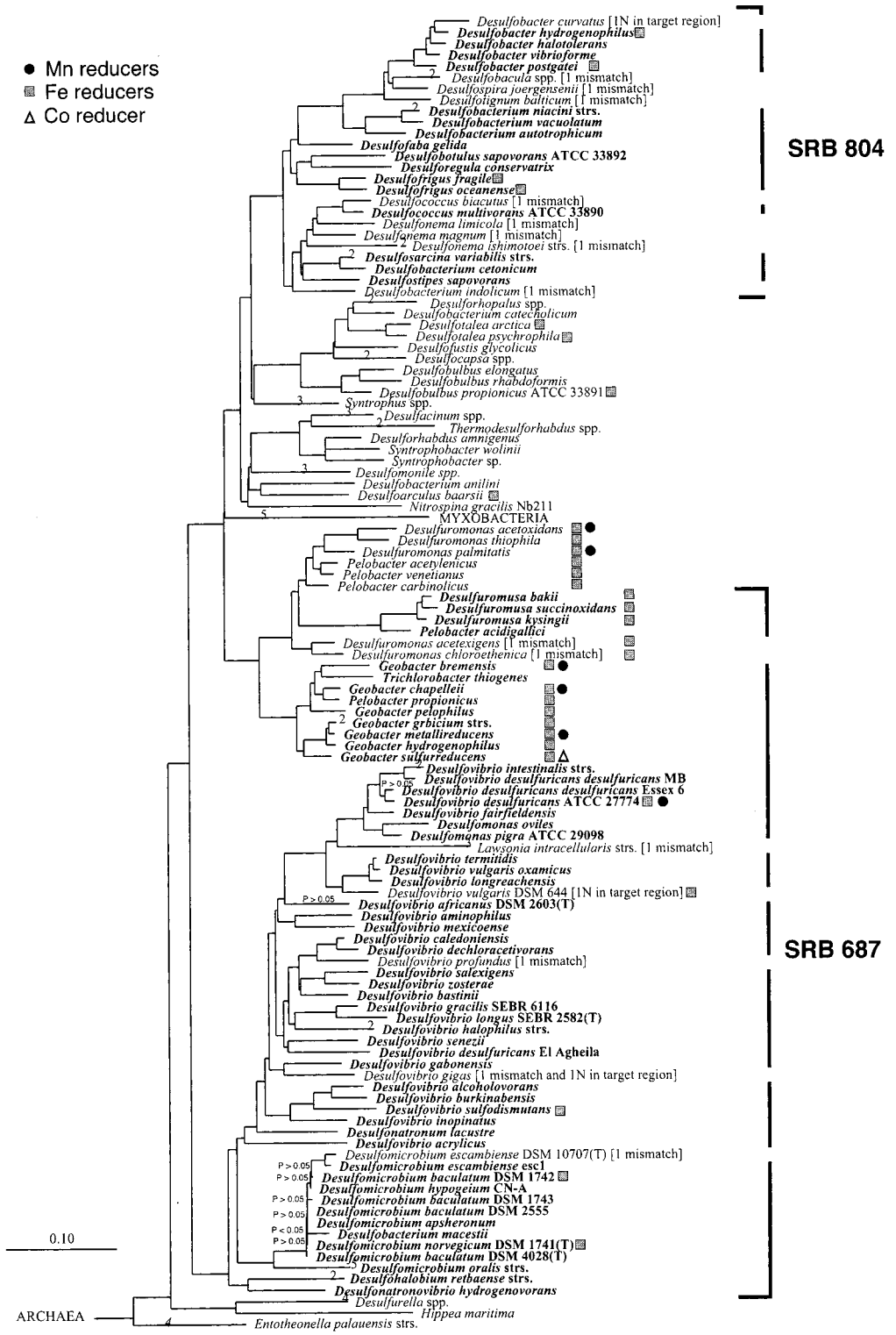

FIGURE 6. 16S rDNA phylogeny of δ proteobacteria. δ proteobacterial probe coverage. Species known to reduce Mn, Fe, and/or Co are indicated (*69*–*72*). The tree includes all relatively full-length δ proteobacterial sequences available (as of December 2000) except that only a few representative *Myxobacteria* sequences were included, as none of them are covered by the probes used or known to reduce metals. The tree was constructed using FastDNA ML (*64*), including only positions that were similar in 40% or more of the sequences. *Entotheonella palauensis* strs., *Desulfomonas oviles*, and *Desulforegula conservatrix* sequences were then added by maximum parsimony. All branch lengths computed by ML were significant ($P < 0.01$), with the exceptions indicated. Numbers above some branches indicate the number of species included in that branch. The scale bar represents 0.1 base changes per position.

the three domain probes (bacterial, eukaryotic, and archaeal). In general, the domain summation ranges between 70 and 175% of the universal probe (Figure 5b), with the exception of a very low summation (<10%) at 5 m and a high summation (220%) at 10 m. Five and 10 m were both depths of minimal RNA recovery, so these poor domain summations may reflect uncertainties in the measurement of extremely small amounts of nucleic acid. Bacterial SSU rRNA accounts for most hybridization at all depths, with a peak between 5 and 10 m. Eukaryotes account for 20–40% of universal probe hybrid-

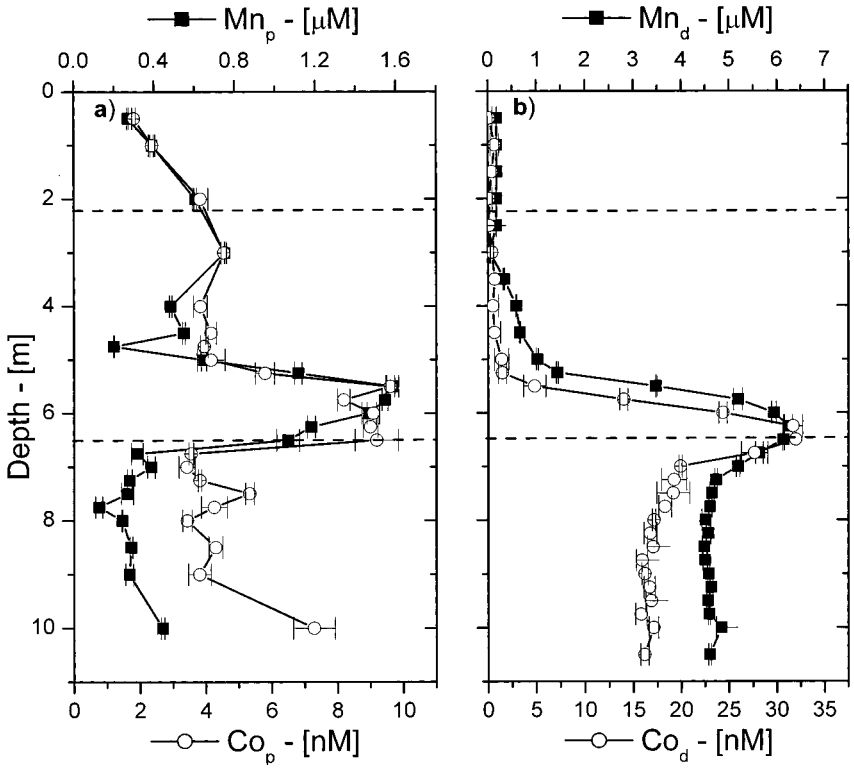

FIGURE 7. Direct evidence of the interaction between Co and Mn in the water column of Paul Lake: (a) Mn_p and Co_p on August 3 and (b) Mn_d and Co_d on August 15. Mn_p and Co_p were below detection limit on August 15. The particulate fraction was collected using the filter digestion method. The dashed lines indicates the location of the chemocline.

ization between 5 and 6 m, where oxygen is still present, but less than 5% in the anoxic zone. Archeal abundance was low at all depth intervals inspected (Figure 5a). The highest absolute abundance was observed at the surface of the lake (ca. 1 ng mL^{-1}), accounting for about 5.4% of total rRNA (Figure 5b). Although high relative abundance was observed at the lowest depth inspected, this was a region of very low biomass (Figure 5a). In general, the Archaea do not appear to be dominant participants in the biogeochemistry of this water column.

The concentration of SSU rRNA targeted by the δ proteobacterial probes (S-F-Dsv-0687-a-A-16 and S-*-Dsb-0804-a-A-18) peaks between 6 and 10 m (Figure 5c), in the region of MnO_x (6 m), iron oxide (7 m, not shown), and SO_4^{2-} (8 m) reduction (see Figure 1). In addition, S-*-Dsb-0804-a-A-18 hybridization displays a smaller peak at 4 m. Interestingly, these two δ proteobacterial probes account for less than 5% of the universal probe hybridization in the anoxic zone, while they account between 10 and 50% of total hybridization in the first 5 m of the water column. This is consistent with a number of other studies that have shown that some δ proteobacteria may be more oxygen tolerant than once believed (*68*). The δ proteobacteria include numerous species able to reduce manganese and/or iron oxides (Figure 6, *69*), and at least one species has been shown to reduce Co (*71*). The *Geobacter*/*Pelobacter*/*Desulfuromonas* group has been the most extensively studied; most of the other species shown in Figure 6 have not yet been tested for metal reduction. Mn-reducing species are among those targeted by both of the δ proteobacterial probes used; thus, these data are consistent with a microbial contribution to MnO_x reduction at 6 m. However, because metal-reducing species are found in many different microbial lineages, they can only be considered indicative of species that might be active. This study has defined the depth intervals of greatest microbial activity and established a foundation for more detailed analyses of population structure in relationship to this process.

The fact that microbial reduction may be responsible for the reductive dissolution of Mn_p in the water column is supported by TEM-EDS data. An investigation during the previous summer showed that MnO_x formed a crust at the surface of some bacteria, hypothesized to be Mn oxidizers (*15*). In contrast, TEM-EDS data collected in August 1996 find no Mn-encrusted bacteria in the chemocline (Figure 3a), supporting the bulk chemistry data showing that Mn^{2+} oxidation was probably slow and that dissolution of MnO_x occurred in the water column during this period. Although it is not possible to infer from these data that microbial reduction occurs in the chemocline, one can speculate that if microbial reduction is involved a consortium of Mn oxidizers and reducers is located in the suboxic zone. From these different measurements, we can conclude that the fast dissolution of MnO_x observed at 5.25 m may only occur by reduction in the presence of organic ligands (*19*), ammonium oxidation (*17*), or microbial reduction (*25*, *26*). These data suggest that the cycling of Mn is not at steady state in the water column of Paul Lake.

Co and Mn Association. On August 3, during the dissolution period, Co_p correlates extremely well with Mn_p. It forms a peak in the lower end of the chemocline with a maximum concentration around 9 nM between 5.5 and 6.5 m (Figure 7a). On August 15, Co_d forms a peak between 5.25 and 7.25 m, with a maximum of 32 nM at 6.25 m (Figure 7b). This peak coincides with the Mn_d peak formed upon dissolution of MnO_x. In addition, Co_p and Mn_p are below detection limit on August 15, confirming their dissolution in the water column.

Data from the water column and the sediment porewaters showed that Co is not significantly brought to the water column from the deep sediment but only recycled from the particulate material at the sediment−water interface and in the water column (*46*). Good correlations were found between Co_d and Mn_d to support this idea (*15*, *46*), and it was suggested that Co is scavenged by MnO_x in the mixolimnion and released in the chemocline when these mineral phases

TABLE 1. Co_p:Mn_p Ratio in the Chemocline on August 3 and August 8, 1996[a]

depth (m) (8/3/96)	5.25	5.5	5.75	6	6.25	6.5
Co_p:Mn_p ratio (%)	0.52	0.61	0.53	0.62	0.76	0.86
depth (m) (8/8/96)	5.2	5.4	5.6	5.8	6	6.5
Co_p:Mn_p ratio (%)	0.66	0.6	0.91	0.98	0.8	1.1

[a] Particulate material was collected using the filter digestion method.

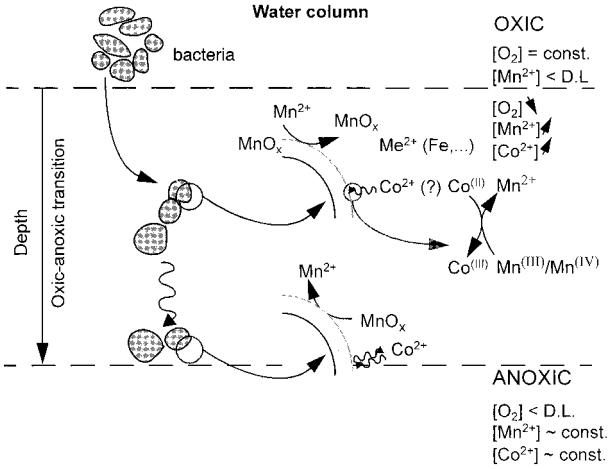

FIGURE 8. Co and Mn cycles proposed to occur in the water column of Paul Lake. Mn crusts are formed at the bacterial surface in the chemocline, and Co is adsorbed or incorporated in the crust. Eventually, oxidation of Co may occur and might be coupled with the reductive dissolution of MnO_x at the bacterial surface. Particles may settle to the lower end of the chemocline, where dissolution of MnO_x releases Mn^{2+} and Co in solution. The wavy lines describe a transport process (i.e., diffusion of Co(II) and sedimentation of particles). D.L. stands for detection limit.

dissolve (*15*). Figure 7 presents clear evidence that Co is associated with MnO_x and is released upon their reductive dissolution during the 2-week period in 1996. In addition, two fine resolution depth profiles of Mn_p and Co_p collected on August 3 and August 8 between 5.25 and 6.5 m (Table 1) show that the Co_p:Mn_p ratio increases with depth, indicating Co is enriched in Mn particles in the lower end of the chemocline. More importantly, the Co_p:Mn_p ratio increases by 20−30% between 5.75 and 6.5 m from August 3 to August 8, suggesting that even though the dissolution of Mn_p releases Co in solution, Co is rapidly recycled and sorbed on Mn_p. The specific sorption of Co by MnO_x has been documented in laboratory and field studies (*33*, *34*), and it is believed that Co(II) is chemically or microbially oxidized to Co(III) at the surface of manganese and hydrous iron oxides (*35*, *36*, *39*, *40*). The depth distributions of particulate and dissolved Co and Mn observed in Paul Lake demonstrate that their limnological biogeochemical cycles are coupled and that the recycling of trace metals at the oxic−anoxic transition can be fast. Although the dissolution mechanism of MnO_x is still unknown, chemical reduction by H_2S and Fe^{2+} can be ruled out in this system because they are not present at the depth of MnO_x dissolution. Microbial reduction, organic ligands or ammonium oxidation are the only known processes that could result in such a rapid reductive dissolution of MnO_x and release of Co in the dissolved phase. This process is probably favored because of the low pH in the suboxic zone. To maintain a steady-state, the formation of the particles must be equally fast; however, this was not the case in July 1996.

The cycling of Mn and Co in the water column of Paul Lake may be inferred from these results (Figure 8). Manganese crusts are formed at the bacterial surface (symbolized by the dark round shapes) in the chemocline, and Co is adsorbed or incorporated in the crust. Eventually, oxidation of Co(II) to Co(III) may occur and might be coupled with the reductive dissolution of MnO_x at the bacterial surface. However, the latter process should have a negligible impact on the reduction of MnO_x since the Co:Mn ratio is below 1%. Manganese-encrusted bacteria may settle to the lower end of the chemocline, where dissolution of MnO_x releases Mn^{2+} and Co in solution. This study shows that a combination of several analytical techniques helps assess biogeochemical processes in aquatic systems. In this regard, the recent emergence of rRNA hybridization molecular probes allows a greater insight into the role of microorganisms when compared to geochemical data.

Acknowledgments

This research was supported by the National Science Foundation (EAR-9815090 to J.-F.G.; DEB-9615356 to J.-F.G. and D.A.S.), the NSF-DOE EMSI program at the Northwestern University Institute of Environmental Catalysis (CHE-9810378), and the Swiss National Science Foundation (Project 20-42250.94 to D.P. and J.-F.G.). We would like to thank J. Runde and R. Hellenthal for the access to UNDERC, L. Méjanelle for helping in the field, H. Percherancier (Cemagref, Fr.) for isolating the Mn oxidizers, and Brett Baker (University of Wisconsin) for sharing unpublished data.

Literature Cited

(1) Morgan, J. J. Ph.D. Dissertation, Harvard University, 1964.
(2) Junta, J. L.; Hochella, M. F., Jr. *Geochim. Cosmochim. Acta* **1994**, *58*, 4985.
(3) Manceau, A.; Gorshkov, A. I.; Drifts, V. A. *Am. Mineral.* **1992**, *77*, 1133.
(4) Wehrli, B.; Friedl, G.; Manceau, A. In *Aquatic Chemistry: Interfacial and Interspecies Processes*; Huang, C. P., O'Melia, C. R., Morgan, J. J., Eds.; ACS Symposium Series 244; American Chemical Society: Washington, DC, 1995; pp 111−134.
(5) Bargar, J. R.; Tebo, B. M.; Villinski, J. E. *Geochim. Cosmochim. Acta* **2000**, *64*, 2775.
(6) Friedl, G.; Wehrli, B.; Manceau, A. *Geochim. Cosmochim. Acta* **1997**, *61*, 275.
(7) Diem, D.; Stumm, W. *Geochim. Cosmochim. Acta* **1984**, *48*, 1571.
(8) Stumm, W.; Morgan, J. J. In *Aquatic Chemistry: Chemical Equilibria and Rates in Natural Waters*; Wiley: New York, 1996; pp 683−686.
(9) Davies, S. H. R.; Morgan, J. J. *J. Colloid Interface Sci.* **1989**, *129*, 63.
(10) Chapnik, S. D.; Moore, W. S.; Nealson, K. H. *Limnol. Oceanogr.* **1982**, *27*, 1004.
(11) Emerson, S.; Kalhom, S.; Jacobs, S.; Tebo, B. M.; Nealson, K. H.; Rossan, R. A. *Geochim. Cosmochim. Acta*. **1982**, *46*, 1073.
(12) Gregory, E.; Staley, T. J. *Appl. Environ. Microbiol.* **1982**, *44*, 2435.
(13) Tebo, B. M.; Ghiorse, W. C.; van Waasbergen, L. G.; Siering, P. L.; Caspi, R. In *Geomicrobiology: Interactions between Microbes and Minerals*; Banfield, J. F., Nealson, K. H., Eds.; Reviews in Mineralogy 35; Mineralogical Society of America: Washington, DC, 1997; pp 225−266.
(14) Davison, W. In *Chemical Processes in Lakes*; Stumm, W., Ed.; Wiley-Interscience: New York, 1985; pp 31−53.
(15) Lienemann, C.-P.; Taillefert, M.; Perret, D.; Gaillard, J.-F. *Geochim. Cosmochim. Acta* **1997**, *61*, 1437.
(16) Van Cappellen, P.; Viollier, E.; Roychoudhury, A.; Clark, L.; Ingall, E.; Lowe, K.; Dichristina, T. *Environ. Sci. Technol.* **1998**, *32*, 2932.
(17) Luther, G. W., III; Sundby, B.; Lewis, B. L.; Brendel, P. J.; Silverberg, N. *Geochim. Cosmochim. Acta* **1997**, *61*, 4043.
(18) Hamilton-Taylor, J.; Davison, W. In *Physics and Chemistry of Lakes*, 2nd ed.; Lerman, A., Gat, J. R., Imboden, D., Eds.; Springer-Verlag: Heidelberg, 1995; pp 1−67.
(19) Stone, A. T. *Geochim. Cosmochim. Acta* **1987**, *51*, 919.
(20) Waite, T. D.; Wrigley, I. C.; Szymezak, R. *Environ. Sci. Technol.* **1988**, *22*, 778.
(21) Stone, A. T.; Morgan, J. *Environ. Sci. Technol.* **1984**, *18*, 617.
(22) Postma, D. *Geochim. Cosmochim. Acta* **1985**, *49*, 1023.
(23) De Vitre, R.; Buffle, J.; Perret, D.; Baudat, R. *Geochim. Cosmochim. Acta* **1988**, *52*, 1601.
(24) Burdige, D. J.; Nealson, K. H. *Geomicrobiol. J.* **1986**, *4*, 361.

(25) Myers, C. R.; Nealson, K. H. *Geochim. Cosmochim. Acta*. **1988**, *52*, 2727.
(26) Lovley, D. R.; Phillips, E. J. P. *Geomicrobiol. J.* **1988**, *6*, 145.
(27) Arakaki, T.; Morse, J. W. *Geochim. Cosmochim. Acta*. **1993**, *57*, 9.
(28) Pedersen, T. F.; Price, N. B. *Geochim. Cosmochim. Acta* **1982**, *46*, 59.
(29) Mucci, A. *Geochim. Cosmochim. Acta* **1988**, *52*, 1859.
(30) Hulth, S.; Aller, R. C.; Gilbert, F. *Geochim. Cosmochim. Acta* **1999**, *63*, 49.
(31) Swift, D. G. *J. Mar. Res.* **1981**, *39*, 375.
(32) Fergusson, J. E. In *The Heavy Elements: Chemistry, Environmental Impact and Health Effects*; Pergamon Press: Oxford, 1990; p 614.
(33) Balistrieri, L. S.; Murray, J. W.; Paul, B. *Limnol. Oceanogr.* **1992**, *37*, 529.
(34) Murray, J. W. *Geochim. Cosmochim. Acta* **1975**, *39*, 635.
(35) Crowther, D. L.; Dillard, J. G.; Murray, J. W. *Geochim. Cosmochim. Acta* **1983**, *47*, 1399.
(36) Lee, B. G.; Fisher, N. S. *Limnol. Oceanogr.* **1993**, *38*, 1593.
(37) Lee, Y.; Tebo, B. B. *Appl. Environ. Microbiol.* **1994**, *60*, 2949.
(38) Moffett, J. W.; Ho, J. *Geochim. Cosmochim. Acta* **1996**, *60*, 3415.
(39) Jardine, P. M.; Taylor, D. L. *Geochim. Cosmochim. Acta* **1995**, *59*, 4193.
(40) Manceau, A.; Drits, V. A.; Silvester, E.; Bartoli, C.; Lanson, B. *Am. Mineral.* **1997**, *82*, 1150.
(41) Elser, M. M.; Elser, J. J.; Carpenter, S. R. *Am. Midl. Nat.* **1986**. *116*, 282.
(42) Carpenter, S. R.; Kitchell, J. F. In *The Trophic Cascade in Lakes*; Carpenter, S. R., Kitchell, J. F., Eds.; Cambridge University Press: Cambridge, England, 1993; pp 15−25.
(43) Johnson, W. E.; Hasler, A. D. *J. Wildl. Manage.* **1954**, *18*, 113.
(44) St. Amand, A. Ph.D. Dissertation, University of Notre Dame, 1990.
(45) Parkin, T. B.; Brock, T. D. *Arch. Microbiol.* **1980**, *125*, 19−27.
(46) Taillefert, M. Ph.D. Dissertation, Northwestern University, 1997.
(47) Taillefert, M.; Lienemann, C.-P.; Gaillard, J.-F.; Perret, D. *Geochim. Cosmochim. Acta* **2000**, *64*, 169.
(48) Fisher, E. *Chem. Ber.* **1883**, *26*, 2234.
(49) Stookey, L. L. *Anal. Chem.* **1970**, *42*, 779.
(50) Kessick, M. A.; Vuceta, J.; Morgan, J. J. *Environ. Sci. Technol.* **1972**, *6*, 642.
(51) Perret, D.; Leppard, G. G.; Muller, M.; Belzile, N.; De Vitre, R.; Buffle, J. *Water Res.* **1991**, *25*, 1333.
(52) Bachhuber, K.; Frösch, D. *J. Microsc.* **1983**, *30*, 1.
(53) MacGregor, B. J. *Curr. Opin. Biotechnol.* **1999**, *10*, 220.
(54) Stahl, D. A.; Flesher, B.; Mansfield, H. R.; Montgomery, L. *Appl. Environ. Microbiol.* **1988**. *54*, 1079.
(55) MacGregor, B. J.; Moser, D. P.; Nealson, K. H.; Stahl, D. A. *Appl. Environ. Microbiol.* **1997**, *63*, 1178.
(56) Alm, E. W.; Oerther, D. B.; Larsen, N.; Stahl, D. A.; Raskin, L. *Appl. Environ. Microbiol.* **1996**, *62*, 3557.
(57) Zheng, D. D.; Alm, E. W.; Stahl, D. A.; Raskin, L. *Appl. Environ. Microbiol.* **1996**, *62*, 4504.
(58) Amann, R. I.; Binder, B. J.; Olson, R. J.; Chisholm, S. W.; Devereux, R.; Stahl, D. A. *Appl. Environ. Microbiol.* **1990**, *56*, 1919.
(59) Hicks, R. E.; Amann, R. I.; Stahl, D. A. *Appl. Environ. Microbiol.* **1992**, *58*, 2158.
(60) Amann, R. I.; Krumholz, L.; Stahl, D. A. *J. Bacteriol.* **1990**, *172*, 762.
(61) Devereux, R.; Kane, M. D.; Winfrey, J.; Stahl, D. A. *Syst. Appl. Microbiol.* **1992**, *15*, 601.
(62) Ghiorse, W. C.; Balkwill, D. L. *Dev. Ind. Microbiol.* **1983**, *24*, 213.
(63) Emerson, D.; Ghiorse, W. C. *Appl. Environ. Microbiol.* **1992**, *58*, 4001.
(64) Strunk, O.; et al. Technische Universität München, München, Germany. http://www.biol.chemie.tu-muenchen.de/pub/ARB/ (accessed 2000).
(65) Baker, B. University of Wisconsin, Madison, personal communication, 2001.
(66) Lienemann, C.-P. Ph.D. Dissertation, University of Lausanne, Switzerland, 1997.
(67) Thamdrup, B.; Dalsgaard, T. *Geochim. Cosmochim. Acta* **2000**, *64*, 4157.
(68) Cypionka, H. *Annu. Rev. Microbiol.* **2000**, *54*, 827.
(69) Lovley, D. R. In *The Prokaryotes*; Dworkin, M., Ed.; Springer: New York, 2000; http://link.springer-ny.com:6335/contents/index.html, Chapter 279.
(70) Lovley, D. R.; Phillips, E. J. P. *Appl. Environ. Microbiol.* **1994**, *60*, 2394.
(71) Caccavo, F., Jr.; Lonergan, D. J.; Lovley, D. R.; Davos, M.; Stolz, J. F.; McInerney, M. J. *Appl. Environ. Microbiol.* **1994**, *60*, 3752.
(72) Finster, K.; Coates, J. D.; Liesack, W.; Pfennig, N. *Int. J. Syst. Bacteriol.* **1997**, *47*, 754.

Received for review May 1, 2001. Revised manuscript received September 18, 2001. Accepted October 10, 2001.

ES010915T